

The Influence of the Quasi-Biennial Oscillation on the Troposphere in Winter in a Hierarchy of Models. Part I: Simplified Dry GCMs

CHAIM I. GARFINKEL* AND DENNIS L. HARTMANN

Department of Atmospheric Science, University of Washington, Seattle, Washington

(Manuscript received 8 September 2010, in final form 23 January 2011)

ABSTRACT

A dry primitive equation model is used to explain how the quasi-biennial oscillation (QBO) of the tropical stratosphere can influence the troposphere, even in the absence of tropical convection anomalies and a variable stratospheric polar vortex. QBO momentum anomalies induce a meridional circulation to maintain thermal wind balance. This circulation includes zonal wind anomalies that extend from the equatorial stratosphere into the subtropical troposphere. In the presence of extratropical eddies, the zonal wind anomalies are intensified and extend downward to the surface. The tropospheric response differs qualitatively between integrations in which the subtropical jet is strong and integrations in which the subtropical jet is weak. While fluctuation-dissipation theory provides a guide to predicting the response in some cases, significant nonlinearity in others, particularly those designed to model the midwinter subtropical jet of the North Pacific, prevents its universal application. When the extratropical circulation is made zonally asymmetric, the response to the QBO is greatest in the exit region of the subtropical jet. The dry model is able to simulate much of the Northern Hemisphere wintertime tropospheric response to the QBO observed in reanalysis datasets and in long time integrations of the Whole Atmosphere Community Climate Model (WACCM).

1. Introduction

Many studies have shown that stratospheric anomalies can affect the tropospheric circulation. In particular, anomalies of the wintertime stratospheric polar vortex have been linked with the northern annular mode (Baldwin and Dunkerton 1999; Polvani and Kushner 2002, hereafter PK02; Limpasuvan et al. 2004). Even though the equatorial stratospheric quasi-biennial oscillation (QBO) is the dominant mode of interannual stratospheric variability in the tropics, its effect on the tropospheric circulation has been less thoroughly investigated.

One way for the QBO to affect the troposphere is through its effect on the polar vortex (Holton and Tan 1980; Hamilton 1998; Baldwin et al. 2001; Coughlin and Tung 2001; Ruzmaikin et al. 2005; Marshall and Scaife 2009). Once the QBO influences the vortex, it could

affect the troposphere just like any vortex anomaly (Baldwin and Dunkerton 1999; Limpasuvan et al. 2004). Another possible pathway is a direct effect of the QBO on the tropical or subtropical troposphere. Crooks and Gray (2005) and Haigh et al. (2005) find that the anomalous QBO winds seemingly arch downward into the subtropical troposphere in a horseshoe-shaped pattern. How this signal is communicated downward through the tropopause has not been fully established, though one possible pathway is through anomalies in convection (Collimore et al. 2003). If such convective anomalies exist, they could affect the extratropics as well, as Ho et al. (2009) found for summertime tropical cyclone tracks in the western North Pacific Ocean (hereafter NP). Simplified two-dimensional models (Dunkerton 1985; Gray and Pyle 1989) have been used to study the meridional circulation (with the focus in the stratosphere) associated with the QBO, and Randel et al. (1999) have examined the meridional circulation from an assimilation of observations, but here we explore simplified modeling to demonstrate how the QBO can impact the troposphere through tropospheric eddies.

Primitive equation models have been used extensively to study the feedbacks between eddies and the mean state in the troposphere (Yu and Hartmann 1993;

* Current affiliation: Johns Hopkins University, Baltimore, Maryland.

Corresponding author address: Chaim I. Garfinkel, Department of Atmospheric Science, University of Washington, Seattle, WA 98195.
E-mail: cig4@atmos.washington.edu

Akahori and Yoden 1997). High-frequency eddies have been shown to reinforce annular mode variability (Feldstein and Lee 1998; Robinson 1996; Lorenz and Hartmann 2001). Recently, the fluctuation–dissipation theorem (FDT) (Leith 1975) has been found to qualitatively describe the response to externally imposed forcing in many cases (i.e., Hartmann et al. 2000; Ring and Plumb 2007, 2008; Gerber et al. 2008). Externally imposed anomalies tend to trigger changes in the natural modes of variability with the largest time scales, and the intraseasonal mode of variability with largest time scale in the extratropical atmosphere is the annular mode.

A few studies have examined the effects of a subtropical or tropical stratospheric forcing on the tropospheric annular modes. Chen and Zurita-Gotor (2008) find that stratospheric zonal wind torques equatorward of 25° and poleward of 30° lead to different signed tropospheric jet shifts. They also find that the response to a 30° torque is not governed solely by a zonally symmetric balanced circulation plus tropospheric eddy feedbacks and friction, inconsistent with a naive (i.e., ignoring the conditions on which the FDT is based) application of the FDT. Haigh et al. (2005), and Simpson et al. (2009, 2011) have examined the effect of lower stratospheric equatorial heating anomalies on tropospheric zonal wind, primarily in the context of how the solar cycle can influence the troposphere. Haigh et al. (2005) find that while a heating anomaly over the pole and over the entire stratosphere leads to an equatorward shift in the jet, an equatorial heating anomaly leads to a poleward shift in the jet. Simpson et al. (2009) use an ensemble of spinup runs to investigate the causality whereby the equatorial heating anomaly leads to the poleward shifted jet. They find that the heating anomaly alters the index of refraction for baroclinic waves near the tropopause, which alters the EP flux propagation pathways and thus EP flux convergence near the tropopause. Zonal wind starts to change as well, thus initiating the annular mode feedback loop. Simpson et al. (2011) find that the response is robust to the introduction of topography and is stronger for tropospheric states with a more equatorward jet (albeit weak, persistent, and narrow) in their control climate, as suggested by the FDT. Although the lower stratospheric temperature and wind anomalies associated with the QBO are more complex than have been previously studied, the results from these studies suggest that the QBO should influence the troposphere even in the absence of an anomalous polar vortex or tropical convection.

We therefore explore how a dry atmosphere responds to QBO momentum forcing. Section 2 discusses the influence of the QBO in observations and in a coupled model and section 3 introduces the simplified model used.

Section 4 discusses the meridional circulation associated with the QBO in the absence of eddies. Sections 5 and 6 then investigate how eddies interact with this direct circulation and influence the troposphere. Three different jet structures are analyzed in order to test the ability of the FDT to explain the effect of the QBO in the troposphere. Section 7 shows that the response is strongest in the jet exit region of a localized subtropical jet, consistent with observations. In Part II of this work (Garfinkel and Hartmann 2011, hereafter Part II) we will examine regional differences between the Pacific and Atlantic sectors in a more complex model that has convection and polar vortex variability.

2. Evidence from observations and coupled models

To provide context for our simplified modeling runs, we first analyze the response to the QBO in Northern Hemisphere winter in the reanalysis record and in a coupled model integration. The 1200 UTC data from the 40-yr European Centre for Medium-Range Weather Forecasts (ECMWF) Re-Analysis (ERA-40) dataset is used from September 1957 until its end (Uppala et al. 2005), and the analysis is extended to August 2007 by using operational 1200 UTC ECMWF Tropical Ocean and Global Atmosphere (TOGA) analysis, yielding 50 years of data. The coupled model integration is a 126-yr run of the Whole Atmosphere Community Climate Model (WACCM) version 3.5. In this run, WACCM is coupled to the land model, the full depth ocean, and the sea ice model of the Community Climate System Model (CCSM; Collins et al. 2006). The simulation is a time-slice run with chemical composition corresponding to 1995, and the time-dependent QBO is imposed as prescribed by the Climate–Chemistry Model Validation Activity (see http://www.pa.op.dlr.de/CCMVal/Forcings/CCMVal_Forcing_WMO2010.html for more information) for the World Meteorological Organization (WMO) Ozone Assessment. See Garfinkel et al. (2010) for more details of this run. The QBO index is the area-averaged zonal wind anomaly from 10°S to 10°N at 50 hPa (results are similar for a 70-hPa QBO), and anomalies are computed as deviations from each calendar month's climatology, for both data sources.

Associated with the easterly phase of the QBO (EQBO) in wintertime of each respective hemisphere is a negative temperature perturbation in the deep tropical stratosphere and a positive temperature perturbation extending from the subtropics to the pole (Fig. 1). The stratospheric temperature perturbations nearly reach the tropopause. The temperature perturbations in the equatorial and subtropical stratosphere move upward when the QBO index is defined at 30 hPa (not shown)

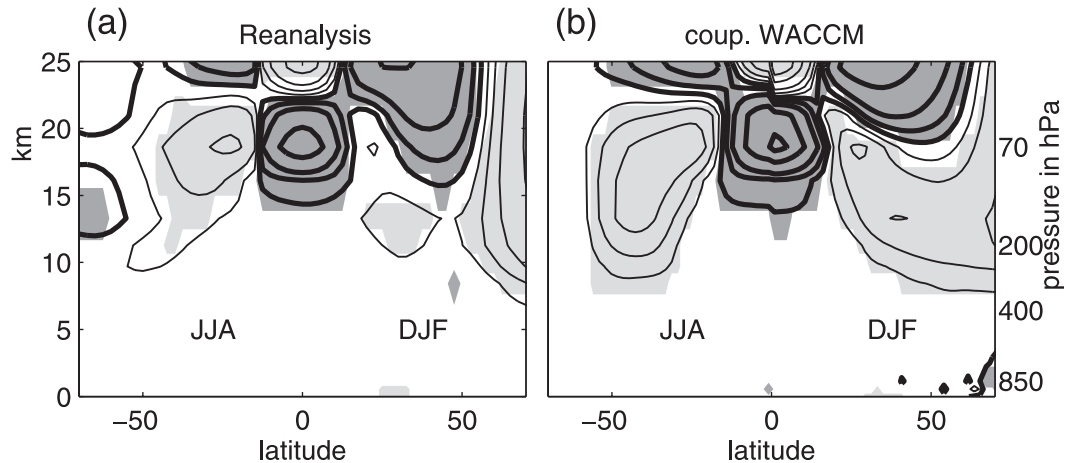


FIG. 1. Cross section of zonally averaged temperature associated with the QBO (EQBO–WQBO) in the reanalysis and coupled WACCM run in winter. Months with zonally averaged zonal wind anomalies at 50 hPa exceeding 5 m s^{-1} are composited as EQBO or WQBO. Contours shown at ± 0.25 , ± 0.75 , ± 1.5 , and $\pm 3 \text{ K}$. The response in June–August (JJA) is shown in the SH, and the response in December–February (DJF) in the NH. A $\log p$ vertical coordinate with $H = 7 \text{ km}$ is used in this and all plots. Negative contours are thick; significant regions at 95% are shaded.

and are present in boreal summer. The temperature anomalies in the stratosphere over the equatorial and subtropical regions are similar for the Pacific and Atlantic basins in both data sources; the QBO is a nearly zonally uniform phenomenon in the stratosphere.

The tropospheric anomalies in different phases of the QBO, however, are zonally asymmetric and vary strongly within winter and between the North Pacific and North Atlantic sectors (Fig. 2). In the Atlantic, the tropospheric response is consistent with the presence of an anomalous stratospheric polar vortex throughout winter [as in Marshall and Scaife (2009), although some indication of a horseshoe-like response in the subtropics is evident especially in October and November (ON)]. In the Pacific, on the other hand, the tropospheric response in ON and February and March (FM) resembles a poleward shift of the subtropical jet, and a weakening of the jet in its climatological position and farther south for EQBO relative to westerly QBO (WQBO). The response is robust to altered definitions of the Pacific basin or to including months with strong QBO winds only. In December and January (DJ), in contrast, the influence of EQBO on the troposphere is neither significant nor consistent between the reanalysis and WACCM.

Our overarching goal is to understand what determines the tropospheric response to different phases of the QBO. During EQBO, the lower stratosphere is anomalously cold near the equator and warm in the subtropics and polar region. But in ONFM, the Pacific jet is shifted poleward from its climatological position, seemingly contradicting Haigh et al. (2005). Can we understand why EQBO leads to a poleward-shifted jet in the Pacific? Garfinkel and Hartmann (2008, 2010) find that the QBO influences

El Niño teleconnections in WACCM and in the reanalysis, but the physical mechanism discussed depends on the QBO influencing the troposphere in an arch or horseshoe-like pattern in the absence of anomalous sea surface temperatures. What is the mechanism whereby the QBO wind anomalies arch downward into the troposphere? Finally, Eichelberger and Hartmann (2007, hereafter EH07) find that eddy feedbacks in the Pacific differ qualitatively between midwinter and early–late winter. Could the same QBO forcing lead to a different response in the Pacific in different wintertime calendar months?

We will show that the QBO can modify tropospheric eddies and shift the tropospheric jet location in a dry primitive equation model. The balanced circulation associated with the QBO can affect the upper troposphere directly. The degree to which EQBO can influence tropospheric eddies is found to be dependent on the variability of the control run with a neutral QBO profile. Because the jets and eddies in the Pacific and Atlantic have different characteristics, the balanced circulation associated with the QBO affects the Pacific and Atlantic sectors differently.

3. The idealized dry model

The Geophysical Fluid Dynamics Laboratory (GFDL) spectral atmospheric dynamical core is used to explore the response to the QBO in the troposphere. The sigma vertical coordinate has 40 vertical levels defined as in PK02; the mesospheric sponge layer follows PK02 except we use a damping coefficient of $\frac{1}{3} \text{ day}^{-1}$; the vertical differencing follows Simmons and Burridge (1981); the bottom boundary is flat so that no stationary planetary waves are

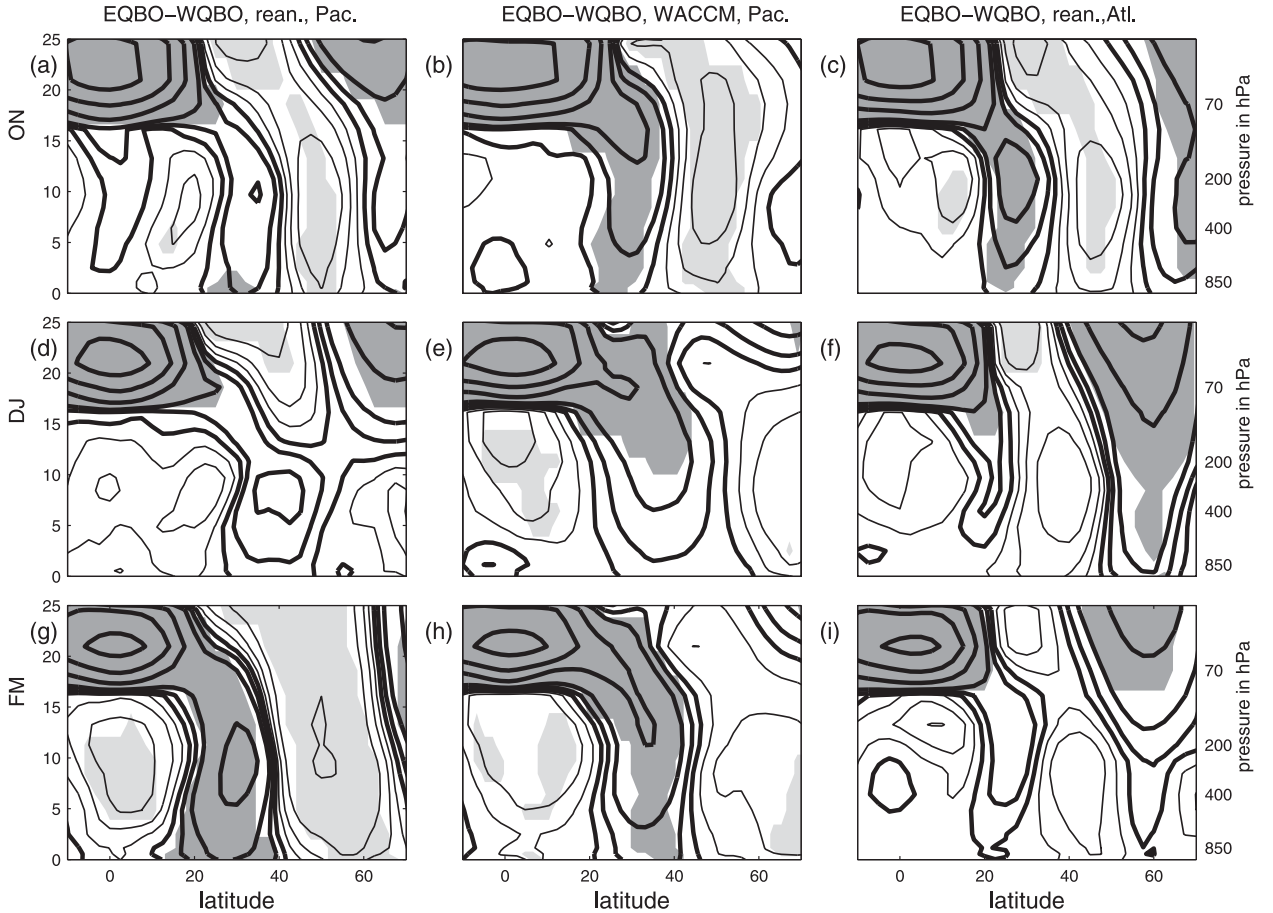


FIG. 2. Cross section of (left) Pacific sector (160°E – 160°W) and (right) Atlantic sector (50° – 10°W) zonal wind associated with the QBO (EQBO–WQBO) in the reanalysis data, and (center) coupled WACCM run in ON, DJ, and FM. The WACCM response in the Atlantic is discussed in Part II. Months with zonally averaged zonal wind anomalies at 50 hPa exceeding 5 m s^{-1} are composited as EQBO or WQBO. Contours shown at ± 0.33 , ± 1 , ± 2 , ± 5 , ± 10 , and $\pm 20 \text{ m s}^{-1}$. For clarity, the SH response is not shown. Negative contours are thick; significant regions at 95% are shaded.

present; ∇^8 hyperdiffusion in the model selectively damps the smallest scale spherical harmonic at a time scale of 0.1 day; and the horizontal resolution is T42. The model output is sampled daily.

Except where specified, the parameterizations follow Held and Suarez (1994, hereafter HS94). The tropospheric temperature relaxation is given by

$$T_{\text{eq}}^{\text{trop}}(p, \phi) = \max \left[200\text{K}, (T_0 - \delta T) \left(\frac{p}{p_0} \right)^{\kappa} \right], \quad (1)$$

where $T_0 = 315 \text{ K}$ (except in section 6), $p_0 = 1000 \text{ hPa}$, and $\kappa = 2/7$, with

$$\delta T = (\Delta T)_y \sin^2 \phi + \epsilon \sin \phi + (\Delta T)_z \log \left(\frac{p}{p_0} \right) \cos^2 \phi, \quad (2)$$

where $(\Delta T)_y = 60 \text{ K}$ (except in section 6 and much of section 4), $(\Delta T)_z = 10 \text{ K}$, and $\epsilon = 0, 5$, or 10 K . In some

runs, a more realistic stratosphere is created following PK02. Above 100 hPa,

$$T_{\text{eq}}^{\text{strat}}(p, \phi) = [1 - W(\phi)] T_{\text{US}}(p) + W(\phi) T_{\text{PV}}(p), \quad (3)$$

where T_{US} is the U.S. Standard Temperature, $T_{\text{PV}}(p) = T_{\text{US}}(p_T)(p/p_T)^{R\gamma/g}$ is the temperature of an atmosphere with a constant lapse rate γ (K km^{-1}), and $W(\phi)$ is a weight function that confines the cooling over the North Pole ($W(\phi) = (1/2)\{1 - \tanh[(\phi - \phi_0)/\delta\phi]\}$) with $\phi_0 = 50$ and $\delta\phi = 10$). The Northern Hemisphere is made the winter hemisphere, but otherwise we follow the formulation in PK02 exactly.

The dry model cannot adequately resolve the equatorial wave dynamics of the QBO. We therefore relax to a QBO wind profile in the tropical stratosphere. The latitudinal structure and formulation of the QBO relaxation in the dry model is analogous to that in the WACCM run from Garfinkel and Hartmann (2010), Matthes et al. (2010), and

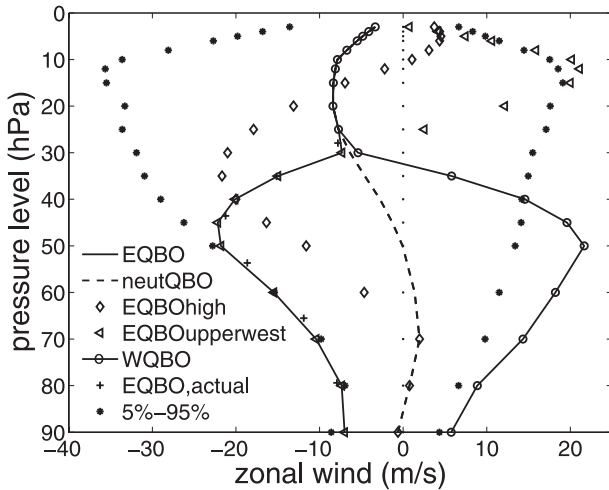


FIG. 3. The QBO wind profiles relaxed. The default east profile (solid line) is identical to the profile used in Garfinkel and Hartmann (2010). The pluses denote the actual wind at the equator 120 days after branching in the J30 case from section 5. Stars represent the 5%–95% range of variability of equatorial zonal wind from May 1953 to April 2007. Dashes indicate the profile relaxed for the control runs. The three profiles with open markers are used to test the robustness of the results.

Part II. Between model σ layers 0.0039 and 0.079 (~ 3.9 and 79 hPa), the winds equatorward of 2° are linearly relaxed toward the specified profile (Fig. 3) with a 10-day time scale. Away from the equator, the linear relaxation time scale increases as $\tau(\phi) = 10e^{(1/2)(\phi/10)^\circ}$ days, where ϕ is latitude. Winds evolve freely poleward of 22° latitude. The QBO for the dry model differs from WACCM in its vertical extent however. The lowest level affected by the QBO relaxation in the dry model is $\sigma = 0.079$ except where indicated, while the next model level (0.096) is not affected at all. In the WACCM runs, the 0.1001 hybrid σ model level has a 20-day relaxation time scale. The default EQBO profile (solid line in Fig. 3) does not have upper stratospheric westerlies like observed QBO profiles. Sensitivity to these upper stratospheric anomalies is weak (see section 4). The tropical stratospheric winds are constrained in all experiments (i.e., in both the control and the EQBO runs).

Three classes of simulations are performed. In the first, the tropospheric response to the QBO in the absence of tropospheric eddy feedbacks is explored (section 4). All dependence on latitude in the HS94 parameterization is removed by fixing terms to their value at the equator [i.e., $T_{\text{eq}} = \max\{200\text{K}, [315\text{K} - (\Delta\theta)_z \log(p/p_0)](p/p_0)^k\}$ and $k_T = k_a + (k_s - k_a) \max[0, (\sigma - \sigma_b)/(1 - \sigma_b)]$; definition of terms is identical to HS94]. These changes remove any meridional gradients in the HS94 parameterizations and thus preclude baroclinic eddies. To speed up model integration, high model

levels are eliminated so that only one vertical level is present above $\sigma = 0.00545$.

In the second class of simulations, the tropospheric response to the QBO when baroclinic eddies are present is explored (section 5). We start with a control run where we relax to climatological winds in the tropical stratosphere (dashes in Fig. 3). We then branch off from this control run at 35-day intervals, impose an EQBO relaxation in the tropical stratosphere, and run the model for another 120 days. No fewer than 50 branch runs are examined for each case. Only the segments of the control run common to the EQBO branch runs are used when computing the response to EQBO. The influence of jet latitude on the tropospheric response to the QBO is explored by comparing the response to the QBO for two different jet locations. In the first configuration, the time mean tropospheric jet peaks near 40°N and has an annular mode with persistence time scale less than 100 days (the stratosphere temperature relaxation profile is isothermal and follows HS94; herein it is denoted J40). Because all model settings are hemispherically symmetric in the J40 case, each hemisphere is treated as an independent degree of freedom. In the second configuration, the time mean jet peaks near 30°N and the annular mode persistence time scale is less than 100 days ($\gamma = 0$ in the PK02 formulation, denoted J30). The key difference in jet location between the two cases likely arises because the PK02 formulation has a lower tropopause, which leads to an equatorward-shifted jet (Gerber and Polvani 2009; Williams 2006). By comparing the response to identical QBO winds in these configurations, the role of the control climate’s mean jet location (which differs between the Atlantic and Pacific sector) in communicating the QBO signal to the troposphere is explored.

In the third class of simulations, the tropospheric response to the QBO in the presence of a tropical heat source is examined (section 6). The tropical heating is slightly changed from EH07 and is specified as

$$Q(p, \phi, \lambda) = Q_0(A + B \sin \lambda) \exp \left[- \left(\frac{\phi - \phi_0}{\phi_w} \right)^2 \right] \times \sin \pi \left[\ln \left(\frac{p}{p_s} \right) / \ln \left(\frac{p_0}{p_s} \right) \right], \quad (4)$$

for $p > 200$ hPa only with $p_0 = 180$ hPa, $Q_0 = 4$ K day $^{-1}$, $\phi_0 = -6^\circ$, and $\phi_w = 4.5^\circ$. EH07 find that tropical heating of this form leads to a stronger subtropical jet that more closely resembles the North Pacific jet in midwinter than a model without tropical heating; this simulation is denoted STJNP, for North Pacific-like subtropical jet. The addition of the heat source while maintaining $(\Delta T)_y$ at 60 K increases the equator to pole temperature gradient, so $(\Delta T)_y$ is reduced to 40 K and

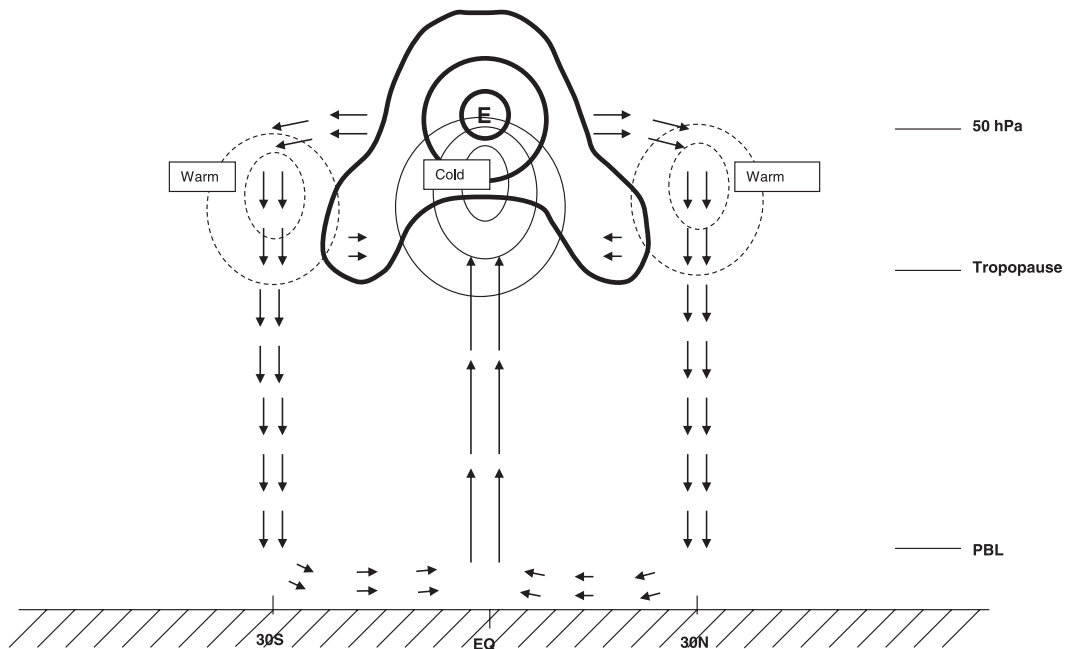


FIG. 4. Schematic of the zonally averaged circulation associated with the QBO in the absence of eddies. Arrows denote the mass weighted circulation. Thick (thin) contours are for zonal wind (temperature). All features, except for the easterly maxima at the equator, are a response to the EQBO winds rather than resulting directly from the externally imposed torque. The Coriolis force implies that part of the return circulation to the equator will occur by the downward-arching zonal wind anomalies above the tropopause, and momentum conservation implies that part of the return circulation to the equator will occur in the PBL.

T_0 lowered to 305 K [Eq. (1)]. Table 2 lists all cases run for the second and third class of simulations. In the second and third classes, an EOF analysis of the $\sqrt{\cos(\phi)}$ weighted zonally averaged surface pressure is performed to diagnose variability.

4. Balanced zonally symmetric response to the QBO

We first discuss the underlying dynamics of the meridional circulation of the QBO and then discuss model runs in which eddy feedbacks are not present.

a. Underlying dynamics

The zonal wind anomalies in the equatorial stratosphere associated with the QBO are subject to thermal wind balance. For QBO variations centered on the equator, thermal wind balance is approximated as

$$\frac{\partial u}{\partial z} \sim \frac{R}{H\beta} \frac{T}{L^2} \quad (5)$$

(Andrews et al. 1987, chapter 8.2), where u is the zonal wind, z is log-pressure height, R is the gas constant for dry air, H is the scale height used in the log-pressure coordinates, T is the temperature anomaly, L is the meridional scale of the circulation, and β is the

latitudinal derivative of the Coriolis parameter. EQBO winds therefore require a cold temperature anomaly at the equator below the peak tropical easterlies to maintain geostrophic balance.

This temperature anomaly is produced by adiabatic expansion associated with upward vertical motion (see the idealized schematic in Fig. 4). This vertical motion near the equator must be balanced by meridional motion diverging from the equator above the temperature anomalies to satisfy mass continuity. If the background state is hemispherically symmetric, half the mass circulation occurs in each hemisphere. This meridional motion will then lead, through the Coriolis force, to a maximum in zonal wind near 30° of the opposite sign to the tropical winds. The secondary zonal wind maximum will be near the location where the meridional motion becomes zero, just like in an axisymmetric Hadley cell.¹

¹ In the absence of eddies, easterlies extend to near the boundary of where the zonal wind relaxation is imposed. In the presence of eddies (and in the actual atmosphere), wave breaking from a variety of wave sources determines the poleward boundary of the easterlies and the subsequent latitude of the secondary subtropical zonal wind maximum. For example, eddy momentum flux convergence determines the latitude (and even the existence) of the secondary maximum in the STJNP case in Figs. 9 and 10.

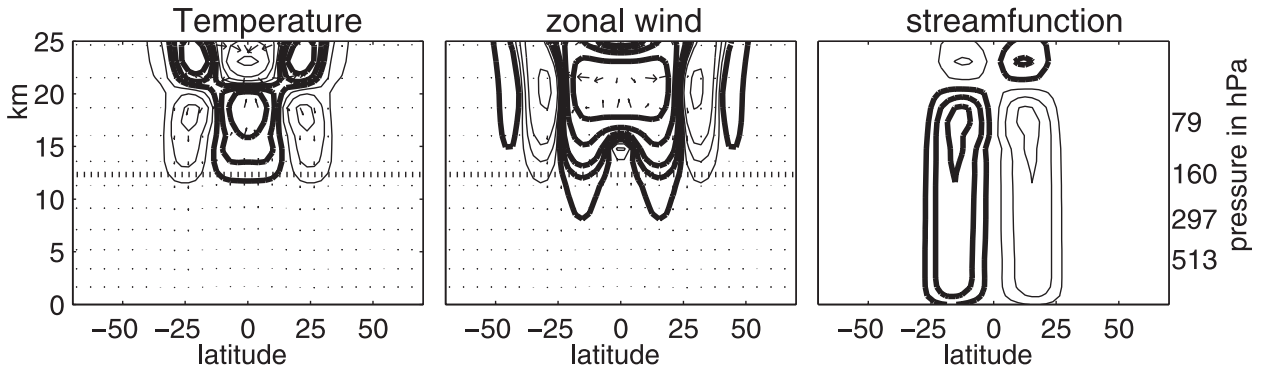


FIG. 5. Zonally averaged (left) temperature, (middle) zonal wind, and (right) streamfunction averaged from days 200 to 600 after the EQBO relaxation is turned on for case A [(case 2 – case 1) in Table 1]. The 200-K contour (i.e., the tropopause) is shown as a dotted line. Contours are shown at ± 0.25 , ± 0.75 , ± 1.5 , and ± 3 K for temperature; ± 0.33 , ± 1 , ± 2 , ± 5 , ± 10 , and ± 20 m s^{-1} for zonal wind; and ± 50 , ± 125 , ± 200 , and ± 275 $\text{m Pa}^{-1} \text{ s}^{-1}$ for streamfunction. Negative contours are thick.

The horizontal mass convergence near 30° will be balanced by downward motion. This downward motion will cause an increase in temperature near 30° . The upward motion near the equator and downward motion near 30° , and their associated temperature anomalies, extend all the way into the troposphere. The meridional circulation thus leads to opposite-signed temperature anomalies at 30° and at the equator. This temperature gradient leads to a zonal wind anomaly near 15° – 20° by thermal wind balance. The stratospheric momentum input associated with the QBO in the tropical stratosphere thus leads to a zonal wind anomaly extending to the tropopause as a self-consistent part of a meridional circulation in thermal wind balance. This qualitative account of the meridional circulation associated with the QBO is consistent with more mathematical treatments in Reed (1964), Plumb (1982), and Plumb and Bell (1982).

The momentum deposited into the system by the EQBO relaxation can be removed by damping in the frictional planetary boundary layer (PBL).² Once the system has reached steady state, any momentum deposited in the QBO region will be balanced by an equivalent amount of momentum removal in the PBL. The meridional circulation set up to balance the QBO momentum forcing thus includes a weak cell that extends to the PBL.

b. Model runs

To illustrate this meridional circulation, Fig. 5 shows the difference in zonally averaged zonal wind, temperature,

and streamfunction between a run with a neutral QBO profile in the stratosphere and an EQBO profile in the stratosphere [(EQBO – neutQBO); i.e., case 2 – case 1 in Table 1]. Upward motion at the equator and downward motion off the equator (implied by the streamfunction) are required to provide the temperature anomalies in thermal wind balance with the EQBO winds. These temperature anomalies are in thermal wind balance with wind anomalies near 15° , so that the stratospheric zonal wind anomaly directly associated with the QBO extends into the troposphere in an arch or horseshoe-like pattern. The equatorward branch of the meridional circulation is concentrated in two places: immediately above the tropopause and in the planetary boundary layer. The momentum forcing (mass- and area-averaged zonal wind forcing) in the EQBO region is 3% greater than the zonal momentum removal in the boundary layer in the 600-day model integration. The 3% discrepancy arises because the wind anomaly in the troposphere takes longer to develop than the wind anomaly in the EQBO region (i.e., the PBL is still not in steady state after 600 days) and because the nonzero damping of the meridional component of the wind in the PBL is ignored. The meridional circulation associated with stratospheric momentum input extends into the troposphere.

The robustness of the meridional circulation is tested. Relaxing toward an EQBO profile with zonal winds 3 times the default [hereafter $3 \times$ EQBO; Figs. 6b,e; (case 3 – case 1) in Table 1a] leads to a similar increase in the strength of the meridional circulation, though not quite by a factor of 3. To demonstrate the role of friction, the boundary layer friction time scale ($1/k_f$ in HS94) is raised to 50 days from 1 day. The response in the stratosphere resembles that in the control case [Figs. 6c,f; (case 5 – case 4) in Table 1a], but the response in the midtroposphere is *stronger* (though slower to develop) than with

² In the actual atmosphere, if the tropical wave driving of the QBO has no net momentum, the EQBO circulation can close in the upper troposphere or lower stratosphere. Such a circulation implies an even stronger zonal wind horseshoe to the tropopause to maintain thermal wind balance and a stronger externally imposed perturbation on upper tropospheric eddies.

TABLE 1. Different runs performed for understanding the response in the troposphere to the QBO in the absence of eddy feedbacks. The tropospheric stratification is as in HS94, except that in all cases but the last two $\cos\phi$ are set to 1 in the expression for k_T and $(\Delta\theta)_z \log(p/p_0) \cos^2\phi$. In the last two cases, the model is run in axisymmetric mode (only zonally symmetric motion is integrated by the model). All cases have the isothermal stratospheric temperature relaxation in HS94. See Fig. 3 for the QBO profiles used; neutQBO denotes relaxation to the climatological stratospheric winds at the equator.

No eddy feedback runs				
Case	QBO profile	Troposphere temp. (K)	Zonal resolution	Vert. levels
1	neutQBO	$(\Delta T)_y = 0$, no jet	Default T42	30
2	EQBO	$(\Delta T)_y = 0$, no jet	Default T42	30
3	$3 \times$ EQBO	$(\Delta T)_y = 0$, no jet	Default T42	30
4	neutQBOwkfrict	$(\Delta T)_y = 0$, no jet	Default T42	30
5	EQBOwkfrict	$(\Delta T)_y = 0$, no jet	Default T42	30
6	neutQBOto95	$(\Delta T)_y = 0$, no jet	Default T42	30
7	EQBOto95	$(\Delta T)_y = 0$, no jet	Default T42	30
8	EQBOupperwest	$(\Delta T)_y = 0$, no jet	Default T42	30
9	halfEQBO	$(\Delta T)_y = 0$, no jet	Default T42	30
10	EQBOhigh	$(\Delta T)_y = 0$, no jet	Default T42	30
11	WQBO	$(\Delta T)_y = 0$, no jet	Default T42	30
12	neutQBO $(\Delta T)_y$	$(\Delta T)_y = 60$	Axisymmetric	30
13	EQBO $(\Delta T)_y$	$(\Delta T)_y = 60$	Axisymmetric	30

a $3 \times$ EQBO profile with the default friction (Fig. 6e). Neither extending the QBO relaxation to the 95-hPa level in the model as in the WACCM QBO parameterization [Fig. 6g; (case 7 – case 6) in Table 1] nor including the upper stratospheric westerlies that are present in observed sheared EQBO profiles [Fig. 6h; (case 8 – case 1) in Table 1; see triangles in Fig. 3] qualitatively changes the circulation. Relaxing to an EQBO profile with zonal winds half of the default [Fig. 6i; (case 9 – case 1) in Table 1] leads to a similar reduction in the strength of the meridional circulation, and relaxing to an EQBO profile shifted upward [Fig. 6j; (case 10 – case 1) in Table 1; see diamonds in Fig. 3] results in an upward-shifted meridional circulation. The response to WQBO winds is opposite that of EQBO winds [(case 11 – case 1) in Table 1; Fig. 6k; see circled solid line in Fig. 3]. Doubling the vertical resolution and allowing meridional gradients in the parameterizations for k_T and the tropospheric stratification [while holding $(\Delta T)_y = 0$ K and strongly damping eddies] does not change the response (not shown). Setting $(\Delta T)_y = 60$ K but running the model in axisymmetric mode does not qualitatively change the response [Fig. 6l; (case 13 – case 12) in Table 1]. Differences do exist in the equatorial upper troposphere, but anomalies in the deep tropics do not project onto the dominant mode of variability and likely have no impact on the extratropical response in

such a model. These differences are much smaller when the model is run in axisymmetric mode and $(\Delta T)_y = 0$ K (not shown). A more fundamental understanding of downward control in the deep tropics, which might explain the differences in the deep tropics, is beyond the scope of this paper. The circulation in thermal wind balance with the EQBO forcing in the absence of eddy feedbacks is referred to as the DIRECT circulation in the rest of this paper.

5. Eddy feedbacks and the response to the QBO

We now show that tropospheric eddies amplify the EQBO DIRECT circulation in both the J30 and J40 configurations (where the time mean jet is at 30° and 40° N, respectively). The model is run for at least 5300 days with the tropical stratospheric winds relaxed toward a neutral QBO profile (the control run). The first 400 days of this run are discarded. We then branch off the instantaneous atmospheric state at 35-day intervals of the control run, relax to an EQBO profile, and run the model for an additional 120 days. At least 70 ensemble members are created for each configuration of the model, and each ensemble member is considered to be an independent sample. The number of ensemble members for each run can be found in Table 2. We thus create an ensemble of the transient response to EQBO relaxation. The robustness of our QBO results is investigated by repeating the same branch experiments but with lower stratospheric winds relaxed to the $3 \times$ EQBO profile. See section 3 for additional methodological details.

We begin by discussing the variability and mean state of the control runs. In both cases, the first EOF of variability of the control run is well separated from all other EOFs and comprises a north–south shift (Fig. 7). The time mean jet is located in the node of the first EOF's dipole, so that in alternate phases of the first EOF, eddies (especially high-frequency eddies) drive the jet equatorward and poleward (Fig. 7). The climatological eddy heat and momentum flux is qualitatively similar in J40 and J30 but is stronger in the J40 case.

The FDT has recently been applied to the response of an annular mode to external forcing. The FDT implies that 1) the response to the imposition of the EQBO relaxation is strongest in cases where the DIRECT circulation of the QBO projects most strongly onto the control climate's annular mode, and 2) the response is strongest when the annular mode persistence time scale is largest. In the cases examined (J40 and J30), the mean jet location varies from 30° to 40° N but the annular mode time scale is nearly constant at ~ 75 days (Fig. 7). Even though application of the FDT requires that the

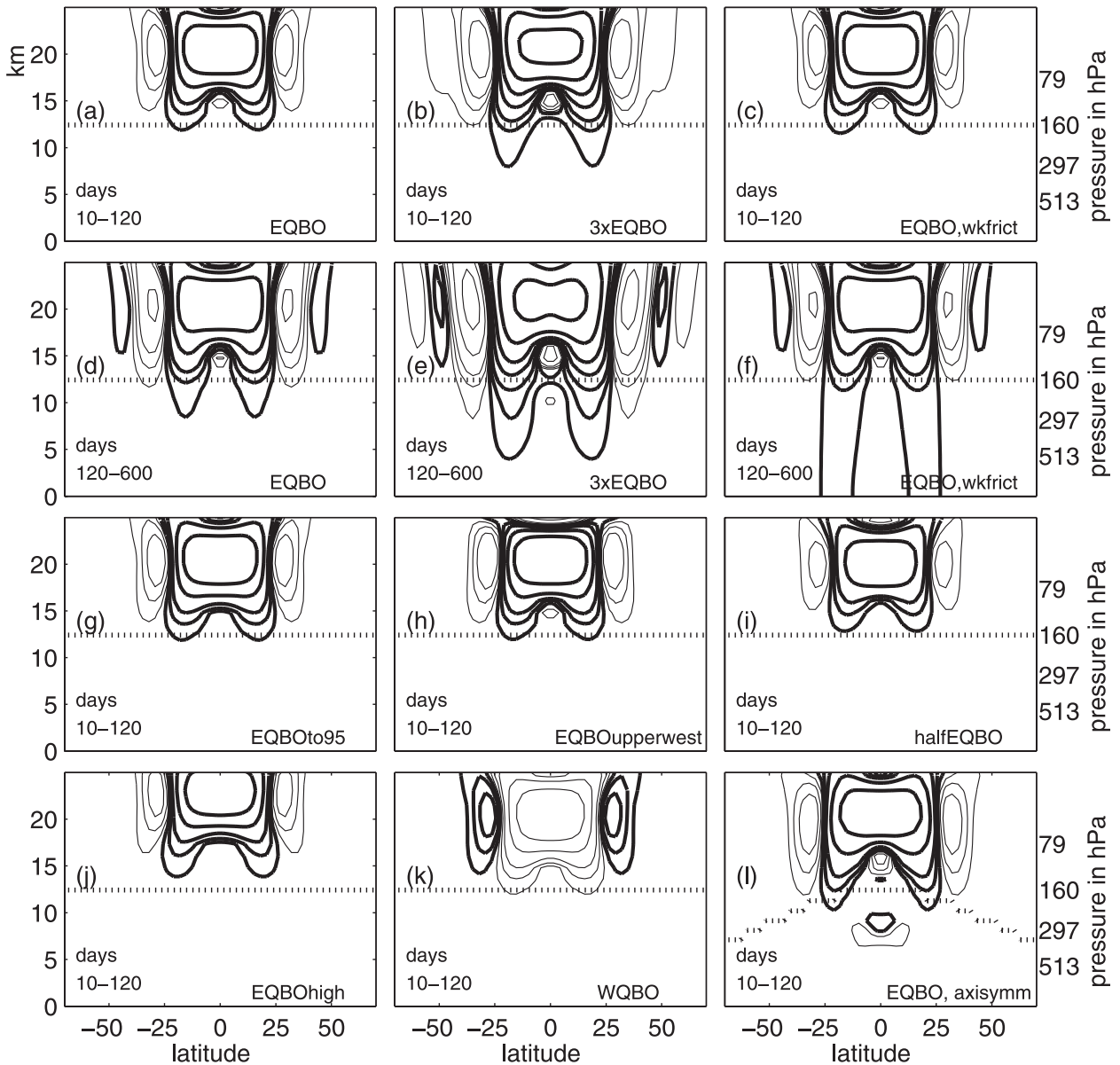


FIG. 6. Difference between EQBO and neutral QBO for different cases. The days of the integration over which the response is averaged are shown in each subplot. (a),(d) Default case in Fig. 5; (b),(e) as in (a),(d), but with equatorial QBO winds stronger by a factor of 3; (c),(f) as in (a),(d), but with less friction. (g)–(l) As in (a), but (g) with the QBO relaxation extended to 95 hPa, (h) with upper and mid-stratospheric westerlies (see Fig. 3), (i) with equatorial winds weaker by a factor of 2, (j) for a QBO profile centered higher in the stratosphere (see Fig. 3), (k) with WQBO winds, and (l) in an axisymmetric version of the model in which a meridional temperature gradient is present. Contours are shown at ± 0.33 , ± 1 , ± 2 , ± 5 , ± 10 , ± 20 , and ± 40 m s^{-1} . The 200-K contour (i.e., the temperature tropopause) is shown as a dotted line.

response and forcing be sufficiently small to remain in the linear regime, we will explore whether the FDT qualitatively describes the response in the troposphere to an identical finite-amplitude EQBO forcing.

The DIRECT zonal wind anomalies of the QBO are plotted with the first EOF of the control climates in Fig. 8. The area-averaged pattern correlation between the first EOF and the DIRECT wind response of the

QBO is shown as well. These are computed from 200 hPa to the surface but are robust to deviations of the correlation region. Because the mean jet position and the annular modes are further poleward for the J40 (Fig. 8a) than for the J30 (Fig. 8b) case, the DIRECT circulation of the QBO projects onto the annular modes in the J30 case much more strongly than the J40 case. We thus expect a weaker response for the J40 case.

TABLE 2. Different runs performed for understanding the response in the troposphere to the QBO in the presence of eddy feedbacks. All cases use 40 vertical levels following PK02. For the control runs, the run length gives the duration (days) after discarding the first 400 days of the run. For the branch runs, the first number is the ensemble size and the second the length of each member of the ensemble (days).

Case	QBO profile	Stratosphere temp.	Eddy runs		
			Tropospheric temp. (K)	Tropical heating	Run length
J40	neutQBO	HS94	$(\Delta T)_y = 60, \epsilon = 0, T_{\max} = 315$	$A = 0, B = 0$	12 250
	EQBO	HS94	$(\Delta T)_y = 60, \epsilon = 0, T_{\max} = 315$	$A = 0, B = 0$	280×120
	$3 \times$ EQBO	HS94	$(\Delta T)_y = 60, \epsilon = 0, T_{\max} = 315$	$A = 0, B = 0$	100×120
J30	neutQBO	PK02, $\gamma = 0$	$(\Delta T)_y = 60, \epsilon = 0, T_{\max} = 315$	$A = 0, B = 0$	7875
	EQBO	PK02, $\gamma = 0$	$(\Delta T)_y = 60, \epsilon = 0, T_{\max} = 315$	$A = 0, B = 0$	180×120
	$3 \times$ EQBO	PK02, $\gamma = 0$	$(\Delta T)_y = 60, \epsilon = 0, T_{\max} = 315$	$A = 0, B = 0$	70×120
STJNP	neutQBO	HS94	$(\Delta T)_y = 40, \epsilon = 5, T_{\max} = 305$	$A = 1, B = 0$	4900
	EQBO	HS94	$(\Delta T)_y = 40, \epsilon = 5, T_{\max} = 305$	$A = 1, B = 0$	140×120
	$3 \times$ EQBO	HS94	$(\Delta T)_y = 40, \epsilon = 5, T_{\max} = 305$	$A = 1, B = 0$	50×120
	WQBO	HS94	$(\Delta T)_y = 40, \epsilon = 5, T_{\max} = 305$	$A = 1, B = 0$	60×120
J30assym	$3 \times$ WQBO	HS94	$(\Delta T)_y = 40, \epsilon = 5, T_{\max} = 305$	$A = 1, B = 0$	60×120
	neutQBO	PK02, $\gamma = 0$	$(\Delta T)_y = 60, \epsilon = 0, T_{\max} = 315$	$A = 0, B = 0.75$	4900
	EQBO	PK02, $\gamma = 0$	$(\Delta T)_y = 60, \epsilon = 0, T_{\max} = 315$	$A = 0, B = 0.75$	120×120
	$3 \times$ EQBO	PK02, $\gamma = 0$	$(\Delta T)_y = 60, \epsilon = 0, T_{\max} = 315$	$A = 0, B = 0.75$	120×120

Figure 9 shows the difference in zonal-mean zonal wind between the control run and the EQBO branch runs for each case. In the first 25 days, the response is restricted to the stratosphere and qualitatively resembles the response shown in Fig. 6 when baroclinic eddies do not exist. In the last 50 days, the altered signal has reached the troposphere and affects the annular mode of the system for the J30 case for the default EQBO profile and both cases for the $3 \times$ EQBO profile. The annular response is weaker in the J40 case, consistent with the weaker projection of the DIRECT circulation of the QBO onto its annular modes.

To confirm that eddies, in particular high-frequency eddies, are responsible for the observed response, Fig. 10 shows the difference in high-frequency (computed with a 7-day high pass ninth-order Butterworth filter) eddy momentum flux convergence $[-(1/a \cos^2 \phi) (\partial \cos^2 \phi (\overline{u'v'}) / (\partial \phi))]$ between the control run and the branch run in the first 90 days after branching for the J30 case. As expected, the eddy momentum flux forcing projects strongly onto the annular modes and the tropospheric response to the QBO. Wavenumbers 6–10 are most important for the response (not shown). The high-frequency eddy momentum flux convergence responds immediately after branching, but not until around day 40 do the eddies consistently modify the circulation. Eddies throughout the upper troposphere and not just near the tropopause are important even in the earliest stage of the tropospheric response.

The quasigeostrophic index of refraction (Andrews et al. (1987, p. 240) can be used to diagnose the preferred direction of Rossby wave propagation. Waves propagate within regions of positive index of refraction and

propagate toward regions of larger index of refraction. To diagnose whether Rossby wave propagation is affected by the QBO, the index of refraction is computed both for the mean state of each control run and for the DIRECT wind and temperature anomalies of the QBO added onto the mean state. For Rossby waves with wavenumbers between 5 and 10 and phase speeds between 5 and 15 m s^{-1} , equatorward propagation is enhanced (i.e., the index of refraction increases equatorward of the jet maximum) and poleward propagation is suppressed (e.g., the dashed line in Fig. 11a is closer to zero near 40°N than the solid line; eddies propagating poleward are therefore more likely to turn rather than break on the poleward flank of the jet), consistent with the momentum flux convergence anomalies in Fig. 10. EQBO wind anomalies enhance equatorward eddy propagation in the lowermost stratosphere.

Our model lacks stationary waves, and we thus do not expect the QBO to influence the stratospheric wintertime polar vortex [e.g., Holton and Austin (1991) for a stratosphere-only model]. To confirm that changes in the polar stratosphere in our integrations do not lead to the changes in the troposphere, the area-averaged polar temperature from 70°N and poleward and for 70 to 150 hPa is computed for each case. Lower stratospheric polar temperatures are not changed by the QBO in the J30 case. In the J40 case, in which there is no winter hemisphere, they are about 1 K warmer in the presence of EQBO winds and nearly 2 K warmer in the presence of $3 \times$ EQBO winds. Variability in the polar regions is not leading to the changes in the troposphere in our model integrations.

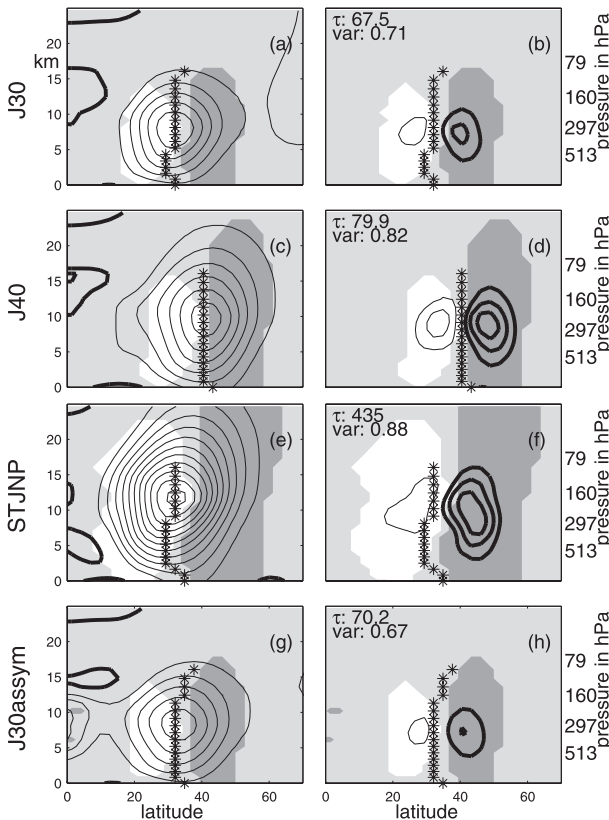


FIG. 7. Mean wind and variability for the cases discussed. (left) Time-mean, zonal-mean zonal wind (contours and stars for jet maximum) with contour interval of 5 m s^{-1} . (right) Projection of the normalized first PC of zonally averaged surface pressure variability onto the high-frequency momentum flux convergence, with a contour interval of $0.5 \text{ m s}^{-1} \text{ day}^{-1}$. The zero contour is omitted in all plots. Both plots also show the regression of the first PC of zonally averaged surface pressure variability onto the zonally averaged zonal wind anomalies in shading. Regions with zonal wind anomalies exceeding $\pm 2 \text{ m s}^{-1}$ for a 1 standard deviation anomaly of the first PC are white and dark gray. The fraction of the variance associated with the first PC and its e -folding persistence time scale are also shown.

Additional runs were also performed but details are not shown for brevity. The quasi-steady (i.e., mean of a long time integration) tropospheric response to EQBO stratospheric forcing resembles the response in days 70–120 in Fig. 9. The response to EQBO winds in the J30 case but at T85 resolution is qualitatively similar though weaker than that shown here; the mean jet position was farther north and the persistence time scale was around 45 days, consistent with the weakened response. The response to EQBO winds centered higher in the stratosphere is qualitatively similar to, albeit weaker than, the response for the default profile (open diamonds in Fig. 3). The response to EQBO winds is also weaker in the presence of a polar vortex [$\gamma = 2$ and $\epsilon = 10 \text{ K}$, the case with the bimodal wind distribution in Chan and Plumb

(2009)]. The QBO does not affect polar cap temperatures in this case either. Even though the annular mode persistence time scale of the control run exceeds 200 days in this case (Chan and Plumb 2009), the projection of the DIRECT EQBO circulation onto the annular modes of the control run is weaker than for the J30 case, potentially explaining the weakened response. The response in the troposphere to WQBO winds (circled solid line in Fig. 3) is, to zeroth order, opposite the response to EQBO winds. QBO winds consistently incline the troposphere toward one phase of its annular mode, and the response is strongest when the DIRECT anomalous winds project most strongly onto the annular modes of the unperturbed climate. Hence our nonlinear model is consistent with the response suggested by the FDT.

6. Response of a strong subtropical jet to the QBO

The influence of the QBO on the troposphere in the Pacific appears different between midwinter and early and late winter (see section 2). We therefore investigate the influence of the QBO on a jet that resembles the North Pacific jet in midwinter. The Pacific subtropical jet is strongest in midwinter, and its variability resembles a pulsing of the jet in one phase and a poleward shift in the other, rather than a north–south shifting (EH07). EH07 find that adding tropical heating concentrated in the tropics to a dry dynamical core strengthens the Hadley circulation and leads to such a shift in the properties of the jet. We therefore explore the response to EQBO wind anomalies in our model in the presence of such a tropical heating source.

Before we discuss the tropospheric response to EQBO winds in such a model configuration, we present some diagnostics of the eddies in the control run. The total lower tropospheric heat flux is little changed upon the addition of the tropical heat source and reduction of $(\Delta T)_y$ to 40 K; hence, $(\Delta T)_y = 40 \text{ K}$ is an appropriate choice. The climatological momentum flux changes qualitatively when such a heat source is added, however, and the high-frequency momentum flux is much reduced (not shown but like EH07). The zonal wind anomalies associated with the first principal component time series (hereafter PC) resembles pulsing and a weak equatorward shift of the jet in one phase and a poleward shift in the other phase, as in EH07³ (Fig. 7). The eddy

³ In truth, the zonally averaged zonal wind anomalies associated with the first PC of the J30 jet are not solely a shift in the jet and include some pulsing of the jet as well. The STJNP jet discussed here has a much greater asymmetry between phases in the high-frequency momentum flux convergence and in the zonal wind anomalies, however.

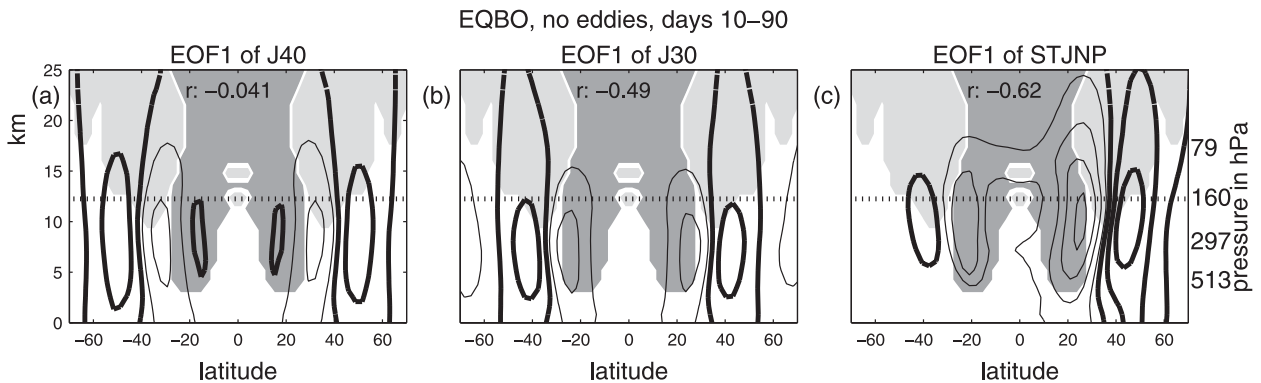


FIG. 8. DIRECT wind anomalies of EQBO and the zonally averaged zonal wind anomalies associated with the first EOF for three different settings of the model. The contours for the zonal wind are ± 1 , ± 3 , ± 5 , ± 7 , ± 9 , and ± 11 m s^{-1} ; regions where the DIRECT zonal wind anomalies exceed 0.05 m s^{-1} are shaded. The area-weighted pattern correlation from 200 hPa to the surface between the two is also shown.

momentum flux convergence anomalies associated with the PC are much stronger in the poleward lobe than the subtropical lobe (Fig. 7), also consistent with EH07. The persistence time scale for the entire run, shown in Fig. 7, blends together these two phases and is likely not meaningful in the context of the FDT. The persistence time scale for a similar run but with a stratospheric polar jet is below 100 days even though the phases of the dominant mode of variability are asymmetric. Much longer runs are necessary before the time scale of a STJNP jet could be precisely known (e.g., Simpson et al. 2011); further investigation is left to future research.

The response of the North Pacific-like subtropical tropospheric jet (STJNP) to EQBO winds is now examined in an ensemble of $3 \times$ EQBO and default EQBO branch runs (see Table 2). Zonal winds intensify in the climatological position of the jet and weaken farther poleward (Figs. 9i–l).⁴ The intensification at the climatological position is particularly strong if we precondition our ensemble for those cases where the jet started out poleward shifted. The response of the troposphere to EQBO winds in the STJNP case is qualitatively different than in the cases from section 5. Instead of an arch of easterlies that descends at 20°N , the easterly wind anomalies form a much broader arch that reaches downward at 45°N (compare Figs. 9i–l to Figs. 9a–h). The DIRECT anomalous zonal wind at 20°N is opposite to the zonal winds in the presence of eddies (see Fig. 8c). FDT cannot be used to even *qualitatively* describe the response of the troposphere in this case.

⁴ An additional integration was performed to examine the influence of EQBO winds on a STJNP tropospheric jet with a stratospheric polar jet present; the tropospheric response to EQBO is nearly identical to that shown here (not shown).

To examine the STJNP case more thoroughly, we conduct a WQBO experiment, and the response is shown in Figs. 9m–p. The westerly wind anomalies descend into the troposphere near 20°N , consistent with the projection of the forcing onto the natural variability and as suggested by the FDT.⁵ Even though the tropical stratospheric winds are reversed in WQBO compared to EQBO, the extratropical tropospheric responses are similar. The similarity in response is consistent with, and might explain, the lack of a response to the QBO in WACCM and the reanalysis during DJ. But the similarity in tropospheric responses to WQBO and EQBO stratospheric winds contradicts a naive application of the FDT.

We now explain why EQBO winds influence a strong subtropical jet in such a manner. We begin by examining eddy momentum flux changes and the associated changes in meridional wave propagation. The eddy momentum flux convergence changes much more quickly, by a larger magnitude, and in the opposite direction to that in the J30 case (Figs. 10d–f). To understand why the eddies propagate in an unexpected direction in the STJNP EQBO case, the quasigeostrophic index of refraction and the potential vorticity gradient \bar{q}_ϕ are computed for the mean state of each control run with and without the DIRECT wind and temperature anomalies of the QBO added on. If the DIRECT EQBO anomalies are added to the climatological flow, a waveguide at upper levels strongly suppresses the equatorward breaking of Rossby waves (i.e., the dashed line on Fig. 11c is well below zero near 17°N). This waveguide inhibits the equatorward

⁵ The WQBO profile is equal and opposite to the EQBO profile, although additional experiments with a more realistic WQBO profile show a similar effect in the troposphere.

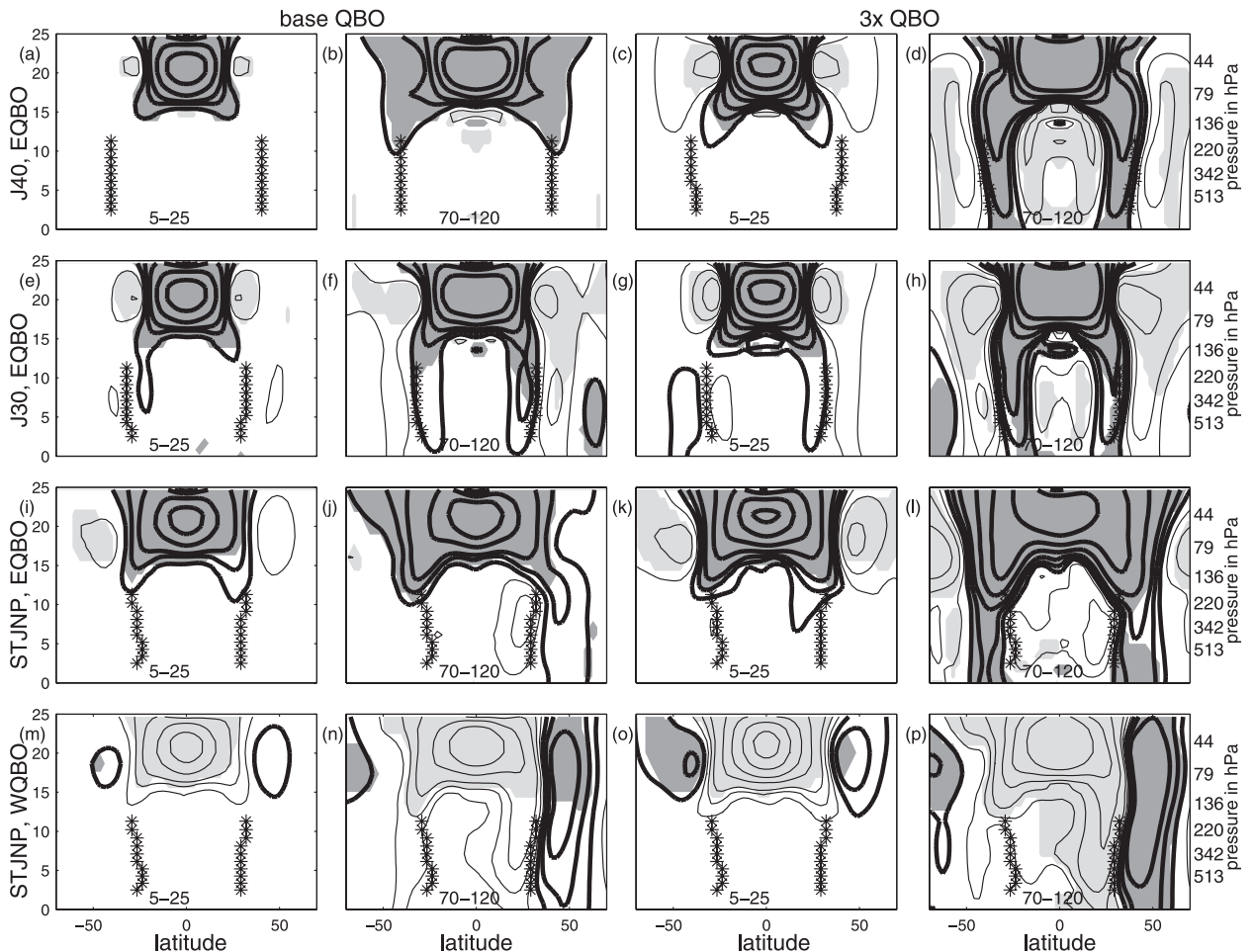


FIG. 9. Response after branching for base QBO profile and $3 \times$ QBO profile for the J40, J30, and STJNP cases. For STJNP, the response with EQBO winds and with WQBO winds is shown. Contours for wind are at $\pm 0.33, \pm 1, \pm 2, \pm 5, \pm 10, \pm 20,$ and $\pm 35 \text{ m s}^{-1}$. Each panel contains the days of the branch run averaged. Negative contours are thick; significant regions at 95% are shaded; stars mark the control run jet maximum.

propagation of eddies necessary to produce easterlies at 20°N and westerlies further poleward that are predicted by naive application of the FDT. Furthermore, \bar{q}_ϕ approaches zero near 15°N if the DIRECT circulation is added onto the climatological winds (dashes in Fig. 11d). In the first few days after branching, the system approaches this marginally stable state (dotted line in Fig. 11c). If eddies were to reinforce the anomaly, as predicted by a naive application of the FDT, the subtropical jet would become unstable, however. The instability would then flux westerly momentum equatorward to smooth out the large curvature in zonal wind, removing the instability. Eddies therefore do not amplify the upper tropospheric wind anomalies forced by the EQBO using the structure of the dominant mode of natural variability. Rather, the eddies support a different, more stable, configuration. In contrast, if the WQBO DIRECT circulation is added onto the STJNP

jet, the jet stays stable. Eddies therefore amplify the DIRECT WQBO circulation by preferentially propagating poleward (Figs. 11e,f). Because of the unique qualities of the STJNP jet, opposite signed external perturbations do not result in opposite signed jet shifts as suggested by the FDT.

The properties of the jet that lead to reduced \bar{q}_ϕ equatorward of the climatological jet position in the presence of the DIRECT EQBO circulation are now explored, as the reduction in \bar{q}_ϕ near 17°N leads to the formation of a waveguide and instability. The contribution from each term constituting \bar{q}_ϕ to the total change in \bar{q}_ϕ is isolated (not shown). We find that the $\partial u/\partial z$ term in $(\rho_0 f^2/N^2)(\partial u/\partial z)$ is most important for the altered \bar{q}_ϕ . By changing $\partial u/\partial z$, the DIRECT QBO arch influences how eddies propagate.

FDT can only be applied when perturbations are sufficiently small so that the response of the system is linear.

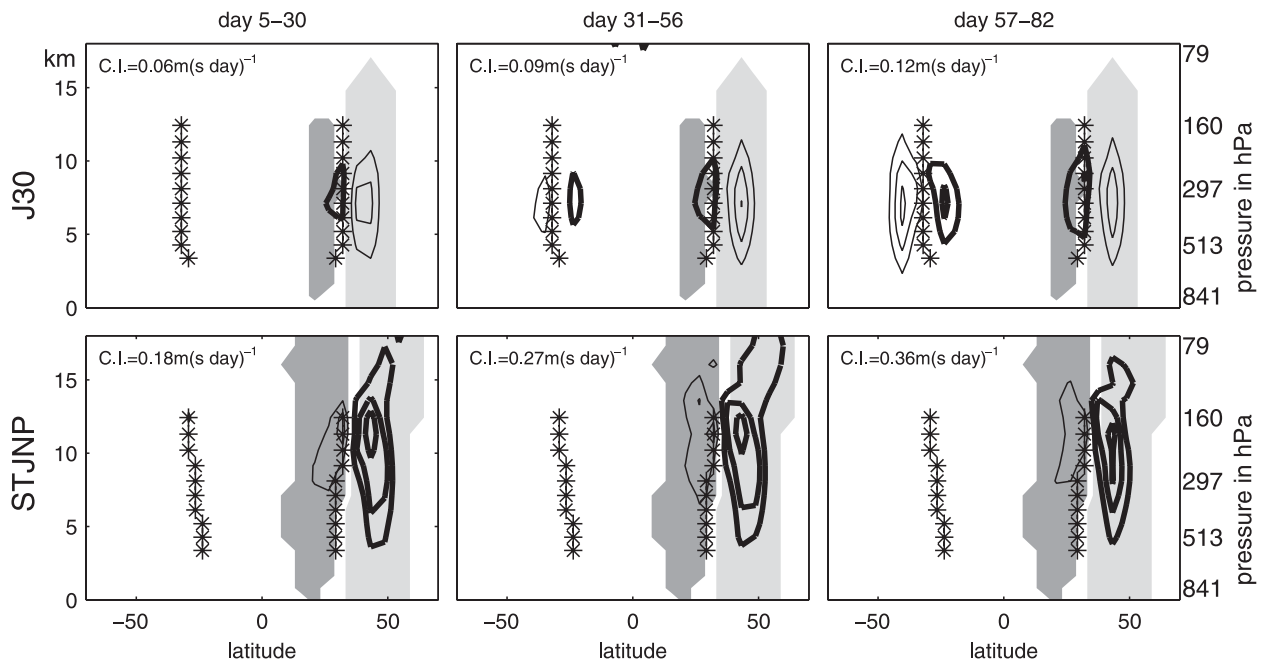


FIG. 10. Anomalous all-wavenumber high-frequency momentum flux convergence for the J30 and STJNP cases after branching with $3 \times$ EQBO winds (contours). Shading denotes regions where the projection of the first PC of 20°N and poleward zonally averaged surface pressure variability onto zonally averaged zonal wind exceeds 2 m s^{-1} . The zero contour is omitted. The vertical axis differs from that in other figures to ease viewing. The contour interval changes among the panels to enhance clarity.

But because the strong subtropical jet case is close to a threshold for instability, even a very small external perturbation, such as that associated with the QBO, can induce a highly nonlinear response. Hence the FDT theory cannot be used to predict the response of this system. In contrast, the J30 and J40 jets are stable; in these cases, the jets shift as suggested by a naive application of the FDT. As the STJNP case represents a strong subtropical jet and is therefore likely relevant to a wintertime Pacific sector jet, the inapplicability of the FDT is particularly noteworthy.

7. Response of a zonally asymmetric jet to the QBO

The model runs in sections 5 and 6 lack stationary waves, and thus modes of variability that involve transfer of energy between the zonally asymmetric mean state and transient eddies. The North Pacific is especially prone to zonally asymmetric variability near the jet exit region (Simmons et al. 1983). We now examine the influence of the QBO on the troposphere in the presence of zonal asymmetries.

Zonal asymmetries are added to the model by setting B in Eq. (4) to 0.75 so that the tropical heating has a zonal wavenumber-1 pattern. Zonal asymmetries are

added to the J30 configuration from section 5 (J30assym in Table 2). The projection of the first PC of zonally averaged surface pressure onto zonally averaged zonal wind still resembles a north–south shifting, and the variance explained by this first EOF is only slightly weaker than when no zonal asymmetries are present (Fig. 7). Eddy feedback is still present. The mean state (Figs. 12a,d) is clearly no longer zonally symmetric, however. The projection of the first PC of nonzonally averaged surface pressure onto zonal wind still resembles an annular mode but is strongest in the jet exit region (not shown); we therefore expect the response to be strongest in this region.

An ensemble of the transient response to EQBO stratospheric winds is created. The response in the upper troposphere is shown in Fig. 12. The influence of the EQBO in the troposphere is robust even in the presence of strong stationary waves. The response in the jet exit region (especially in days 45–75 of the $3 \times$ EQBO run and days 70–120 of the default EQBO run) is stronger than the zonally symmetric response in Figs. 9e–h. The response in the jet exit region is concentrated at and just equatorward of the mean jet position in the control simulation, whereby the subtropical jet is shortened and weakened. The effect of asymmetric heating on a model configuration that also has zonally symmetric heating

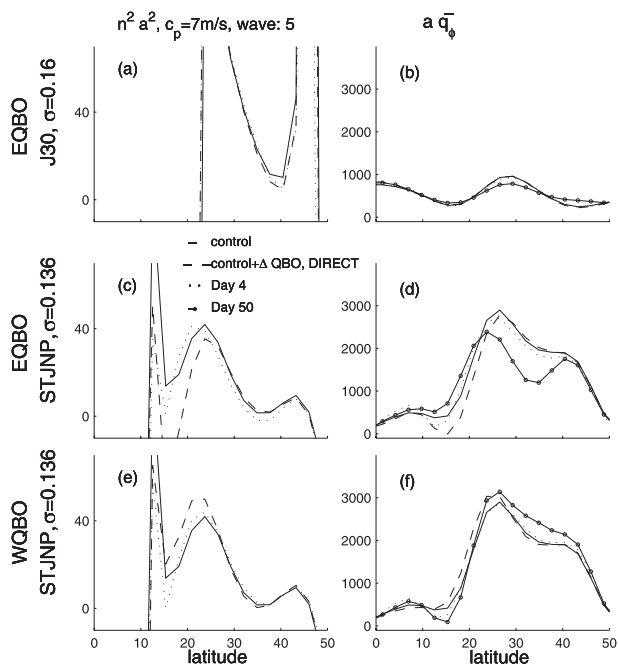


FIG. 11. (left) Index of refraction (multiplied by the earth's radius squared) for wavenumber 5 and zonal phase speed 7 m s^{-1} , and (right) meridional gradient of potential vorticity \bar{q}_ϕ (multiplied by the earth's radius), for the STJNP and J30 cases: (a),(b) EQBO J30; (c),(d) EQBO STJNP; and (e),(f) WQBO STJNP. These are computed for the control run (solid line), the control plus the DIRECT QBO circulation (dashed line), 4 days after branching with QBO winds (dotted line), and 50 days after branching with QBO winds (circled solid line). For clarity, the index of refraction 50 days after branching with QBO winds is not shown. The σ level just above the jet maximum near the top of where eddies break climatologically is shown for each case; results are similar for adjacent levels.

as in section 6 was also investigated; the response to EQBO winds qualitatively resembles that shown in Fig. 12 (not shown). The QBO influences the jet exit region of a subtropical jet, consistent with the FDT and observations.

8. Conclusions

In both the reanalysis record and in a WACCM run, winds are significantly weaker near and south of the climatological jet position in the subtropical Pacific during the easterly phase of the QBO, relative to its westerly phase. The effect is particularly strong in February and March, and to a lesser degree in October and November, when jet variability is more characterized by north–south shifting. In December and January when the subtropical jet is stronger and jet variability is better characterized as a pulsing of jet strength, the effect is, if anything, opposite to that in early and late winter.

To understand why the QBO may have such an influence, a QBO is added to a primitive equation dry dynamical core and the effect on the troposphere studied. QBO momentum anomalies require a meridional circulation to establish thermal wind balance. The zonal wind associated with this circulation arches down to the subtropical troposphere. This circulation is robust to model configuration.

In the presence of eddies, the tropospheric response differs qualitatively depending on the strength and position of the jet. When the dominant mode of variability is a shifting jet, EQBO winds result in a poleward-shifted jet. The response is stronger for a tropospheric jet whose mean position is farther equatorward, as suggested by the fluctuation–dissipation theorem. The response in the model is consistent with the observed response in the Pacific in early and late winter. In the Atlantic, the influence of the QBO on the polar vortex and thereby on the North Atlantic Oscillation is important. The model configuration discussed here does not permit realistic polar vortex variability, however. In addition, the Atlantic tropospheric jet is farther poleward than the Pacific jet (i.e., the Atlantic jet more closely resembles the J40 case, and the Pacific jet more closely resembles the J30 case), which likely also contributes to the weakness of the response to the QBO in the Atlantic from December through March.

In our strong subtropical jet case, both EQBO and WQBO forcing result in an intensification of the jet in its climatological position. Strong subtropical jets react similarly to opposite phases of the QBO, consistent with the change in the index of refraction for Rossby waves and with stability arguments, but not with a naive application of the fluctuation dissipation theorem. In the reanalysis data, the influence of the QBO in the Pacific in midwinter is weak, consistent with results from our model. Finally, the response is magnified in the jet exit region in a zonally asymmetric configuration of the model, as is observed in the Pacific. Strong subtropical jets and weaker jets respond differently to the same QBO forcing in both observations and in the dry model.

A dry model has fundamental limitations on its ability to simulate the actual atmosphere. Specifically, it lacks convection and possible convective feedbacks, and convection may be important for the tropospheric response to the QBO. The model used here also lacks realistic polar vortex variability and realistic stationary waves. Furthermore, the dominant mode of variability in a dry model with no topography explains a much higher share of the total variance than the dominant mode of variability in the observations. It is conceivable that these defects of the dry model preclude an accurate simulation of the influence of the QBO on the troposphere in the atmosphere. Part II of this work will therefore focus on

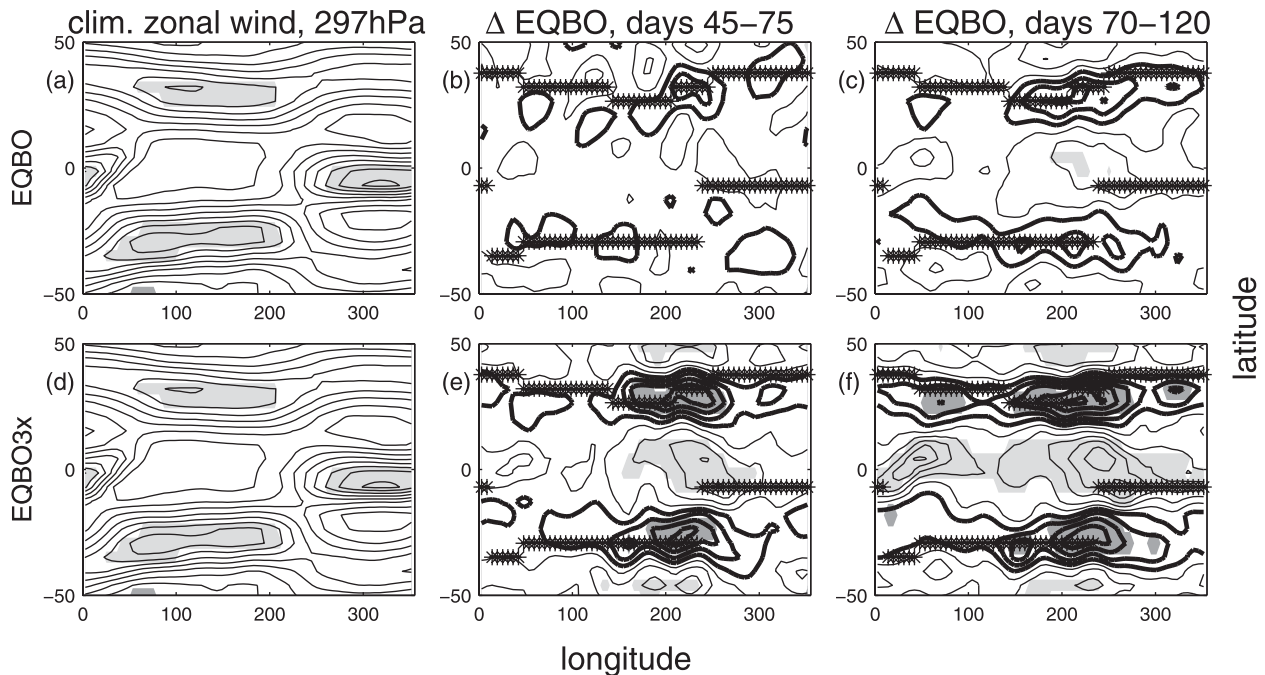


FIG. 12. (a),(d) Mean zonal wind in the control case and (b),(c),(e),(f) response to EQBO—(middle) days 45–75 and (right) days 70–120—at the 297-hPa level for the zonally asymmetric heating cases. For (a),(d), regions with zonal wind below 0 m s⁻¹ (above 30 m s⁻¹) are shaded dark (light) gray, and contours are shown every 5 m s⁻¹. For (b),(c),(e),(f), negative contours are thick; significant regions at 95% are shaded; contours are shown at $\pm 0.5, \pm 1.5, \dots, \pm 5.5$ m s⁻¹; and stars mark the jet maximum at each longitude.

a model that has eddy feedbacks as well as realistic tropospheric stationary waves and parameterized convection. Part II will show that eddies are important for the communication of this signal even in the presence of convection and vortex variability.

Nevertheless, it is remarkable that a relatively simple model like the one used here is capable of qualitatively capturing the observed signal. The sensitivity of the response to the mean state of the unperturbed climate highlights the nonlinearities in the atmospheric system and provides an example where naive FDT thinking can lead one astray. The inapplicability of the FDT to a strong subtropical jet has possible implications for the response of such a jet to external perturbations other than the QBO, such as increased CO₂; further analysis is left for future work.

Acknowledgments. This work was supported by the National Science Foundation under Grant AGS 0960497. We thank Fabrizio Sassi for providing the data from the WACCM 3.5 run, the developers at GFDL for the dry model, Sarah Leibert Garfinkel for producing Fig. 4, and Marc L. Michelsen for assisting our dry model runs. Finally, we wish to thank Peter Rhines, Chris Bretherton, and our especially helpful and conscientious anonymous reviewers, whose comments have helped us improve the manuscript.

REFERENCES

- Akahori, K., and S. Yoden, 1997: Zonal flow vacillation and bimodality of baroclinic eddy life cycles in a simple global circulation model. *J. Atmos. Sci.*, **54**, 2349–2361.
- Andrews, D. G., J. R. Holton, and C. B. Leovy, 1987: *Middle Atmosphere Dynamics*. Academic Press, 489 pp.
- Baldwin, M. P., and T. J. Dunkerton, 1999: Propagation of the Arctic Oscillation from the stratosphere to the troposphere. *J. Geophys. Res.*, **104** (D24), 30 937–30 946.
- , and Coauthors, 2001: The quasi-biennial oscillation. *Rev. Geophys.*, **39**, 179–229.
- Chan, C. J., and R. A. Plumb, 2009: The response to stratospheric forcing and its dependence on the state of the troposphere. *J. Atmos. Sci.*, **66**, 2107–2115.
- Chen, G., and P. Zurita-Gotor, 2008: The tropospheric jet response to prescribed zonal forcing in an idealized atmospheric model. *J. Atmos. Sci.*, **65**, 2254–2271.
- Collimore, C. C., D. W. Martin, M. H. Hitchman, A. Huesmann, and D. E. Waliser, 2003: On the relationship between the QBO and tropical deep convection. *J. Climate*, **16**, 2552–2568.
- Collins, W. D., and Coauthors, 2006: The Community Climate System Model version 3 (CCSM3). *J. Climate*, **19**, 2122–2143.
- Coughlin, K., and K.-K. Tung, 2001: QBO signal found at the extratropical surface through northern annular modes. *Geophys. Res. Lett.*, **28**, 4563–4566.
- Crooks, S. A., and L. J. Gray, 2005: Characterization of the 11-year solar signal using a multiple regression analysis of the ERA-40 dataset. *J. Climate*, **18**, 996–1015.
- Dunkerton, T. J., 1985: A two-dimensional model of the quasi-biennial oscillation. *J. Atmos. Sci.*, **42**, 1151–1160.

- Eichelberger, S. J., and D. L. Hartmann, 2007: Zonal jet structure and the leading mode of variability. *J. Climate*, **20**, 5149–5163.
- Feldstein, S., and S. Lee, 1998: Is the atmospheric zonal index driven by an eddy feedback? *J. Atmos. Sci.*, **55**, 3077–3086.
- Garfinkel, C. I., and D. L. Hartmann, 2008: Different ENSO teleconnections and their effects on the stratospheric polar vortex. *J. Geophys. Res.*, **113**, D18114, doi:10.1029/2008JD009920.
- , and —, 2010: The influence of the quasi-biennial oscillation on the North Pacific and El Niño teleconnections. *J. Geophys. Res.*, **115**, D20116, doi:10.1029/2010JD014181.
- , and —, 2011: The influence of the quasi-biennial oscillation on the troposphere in wintertime in a hierarchy of models. Part II: Perpetual winter WACCM runs. *J. Atmos. Sci.*, in press.
- , —, and F. Sassi, 2010: Tropospheric precursors of anomalous Northern Hemisphere stratospheric polar vortices. *J. Climate*, **23**, 3282–3299.
- Gerber, E. P., and L. M. Polvani, 2009: Stratosphere–troposphere coupling in a relatively simple AGCM: The importance of stratospheric variability. *J. Climate*, **22**, 1920–1933.
- , S. Voronin, and L. M. Polvani, 2008: Testing the annular mode autocorrelation time scale in simple atmospheric general circulation models. *Mon. Wea. Rev.*, **136**, 1523–1536.
- Gray, L. J., and J. A. Pyle, 1989: A two-dimensional model of the quasi-biennial oscillation of ozone. *J. Atmos. Sci.*, **46**, 203–220.
- Haigh, J. D., M. Blackburn, and R. Day, 2005: The response of tropospheric circulation to perturbations in lower-stratospheric temperature. *J. Climate*, **18**, 3672–3685.
- Hamilton, K., 1998: Effects of an imposed quasi-biennial oscillation in a comprehensive troposphere–stratosphere–mesosphere general circulation model. *J. Atmos. Sci.*, **55**, 2393–2418.
- Hartmann, D. L., J. M. Wallace, V. Limpasuvan, D. W. J. Thompson, and J. R. Holton, 2000: Can ozone depletion and global warming interact to produce rapid climate change? *Proc. Natl. Acad. Sci. USA*, **97**, 1412–1417.
- Held, I. M., and M. J. Suarez, 1994: A proposal for the intercomparison of the dynamical cores of atmospheric general circulation models. *Bull. Amer. Meteor. Soc.*, **75**, 1825–1830.
- Ho, C., H. Kim, J. Jeong, and S. Son, 2009: Influence of stratospheric quasi-biennial oscillation on tropical cyclone tracks in the western North Pacific. *Geophys. Res. Lett.*, **36**, L06702, doi:10.1029/2009GL037163.
- Holton, J. R., and H.-C. Tan, 1980: The influence of the equatorial quasi-biennial oscillation on the global circulation at 50 mb. *J. Atmos. Sci.*, **37**, 2200–2208.
- , and J. Austin, 1991: The influence of the equatorial QBO on sudden stratospheric warmings. *J. Atmos. Sci.*, **48**, 607–618.
- Leith, C. E., 1975: Climate response and fluctuation dissipation. *J. Atmos. Sci.*, **32**, 2022–2026.
- Limpasuvan, V., D. W. J. Thompson, and D. L. Hartmann, 2004: The life cycle of the Northern Hemisphere sudden stratospheric warmings. *J. Climate*, **17**, 2584–2596.
- Lorenz, D. J., and D. L. Hartmann, 2001: Eddy–zonal flow feedback in the Southern Hemisphere. *J. Atmos. Sci.*, **58**, 3312–3327.
- Marshall, A. G., and A. A. Scaife, 2009: Impact of the QBO on surface winter climate. *J. Geophys. Res.*, **114**, D18110, doi:10.1029/2009JD011737.
- Matthes, K., D. R. Marsh, R. R. Garcia, D. E. Kinnison, F. Sassi, and S. Walters, 2010: Role of the QBO in modulating the influence of the 11-year solar cycle on the atmosphere using constant forcings. *J. Geophys. Res.*, **115**, D18110, doi:10.1029/2009JD013020.
- Plumb, R. A., 1982: Zonally symmetric Hough modes and meridional circulations in the middle atmosphere. *J. Atmos. Sci.*, **39**, 983–991.
- , and R. C. Bell, 1982: A model of the quasi-biennial oscillation on an equatorial beta-plane. *Quart. J. Roy. Meteor. Soc.*, **108**, 335–352, doi:10.1029/smsqj.45603.
- Polvani, L. M., and P. J. Kushner, 2002: Tropospheric response to stratospheric perturbations in a relatively simple general circulation model. *Geophys. Res. Lett.*, **29**, 1114, doi:10.1029/2001GL014284.
- Randel, W. J., F. Wu, R. Swinbank, J. Nash, and A. O'Neill, 1999: Global QBO circulation derived from UKMO stratospheric analyses. *J. Atmos. Sci.*, **56**, 457–474.
- Reed, R. J., 1964: A tentative model of the 26-month oscillation in tropical latitudes. *Quart. J. Roy. Meteor. Soc.*, **90**, 441–466, doi:10.1002/qj.49709038607.
- Ring, M. J., and R. A. Plumb, 2007: Forced annular mode patterns in a simple atmospheric general circulation model. *J. Atmos. Sci.*, **64**, 3611–3626.
- , and —, 2008: The response of a simplified GCM to axisymmetric forcings: Applicability of the fluctuation–dissipation theorem. *J. Atmos. Sci.*, **65**, 3880–3898.
- Robinson, W. A., 1996: Does eddy feedback sustain variability in the zonal index? *J. Atmos. Sci.*, **53**, 3556–3569.
- Ruzmaikin, A., J. Feynman, X. Jiang, and Y. L. Yung, 2005: Extratropical signature of the quasi-biennial oscillation. *J. Geophys. Res.*, **110**, D11111, doi:10.1029/2004JD005382.
- Simmons, A. J., and D. M. Burridge, 1981: An energy and angular-momentum conserving vertical finite-difference scheme and hybrid vertical coordinates. *Mon. Wea. Rev.*, **109**, 758–766.
- , J. M. Wallace, and G. Branstator, 1983: Barotropic wave propagation and instability, and atmospheric teleconnection patterns. *J. Atmos. Sci.*, **40**, 1363–1392.
- Simpson, I. R., M. Blackburn, and J. D. Haigh, 2009: The role of eddies in driving the tropospheric response to stratospheric heating perturbations. *J. Atmos. Sci.*, **66**, 1347–1365.
- , —, —, and S. Sparrow, 2011: The impact of the state of the troposphere on the response to stratospheric heating in a simplified GCM. *J. Climate*, **23**, 6166–6185.
- Uppala, S. M., and Coauthors, 2005: The ERA-40 Re-Analysis. *Quart. J. Roy. Meteor. Soc.*, **131**, 2961–3012.
- Williams, G. P., 2006: Circulation sensitivity to tropopause height. *J. Atmos. Sci.*, **63**, 1954–1961, doi:10.1175/JAS3762.1.
- Yu, J., and D. L. Hartmann, 1993: Zonal flow vacillation and eddy forcing in a simple GCM of the atmosphere. *J. Atmos. Sci.*, **50**, 3244–3259.